

## Analysis of T-10 Data on Magnetic Island Dynamics Using the TEAR Code

N.V. Ivanov, A.N. Chudnovskiy, A.M. Kakurin, I.I. Orlovskiy

*Nuclear Fusion Institute, RRC «Kurchatov Institute», Moscow, Russia*

E-mail: [ivnick@nfi.kiae.ru](mailto:ivnick@nfi.kiae.ru)

### Introduction

The T-10 tokamak experimental data on the  $m = 2$ ,  $n = 1$  mode locking by the Error Field with the same helicity are analysed with the use of the TEAR code.

The TEAR code [1 - 4] is based on the non-linear Rutherford model [5, 6] in the presence of plasma rotation and the Resonant Magnetic Perturbation (RMP), which simulates the Error Field. The time variations of the toroidal and poloidal rotation velocities of the plasma layer in the vicinity of the resonant magnetic surface are calculated similar to [7 - 9] with the use of the angular motion equations in the toroidal and poloidal directions.

### Experimental Observation of the Mode Locking

T-10 is a tokamak with a circular plasma cross-section. The major and minor radii of the vacuum vessel are  $R = 1.5$  m and  $b = 0.42$  m, the radius of the permanent circular limiter is 0.33 m. The plasma minor radius determined by the position of the movable rail limiter is  $a = 0.27$  m. The experiments are carried out using Ohmic discharges with the toroidal magnetic field  $B_T = 2.4$  T, discharge current  $I_p = 240$  kA, line-average plasma density  $\bar{n}_e = 0.8 \cdot 10^{19} \text{ m}^{-3}$ . The  $m = 2$ ,  $n = 1$  harmonic of the Error Field at the plasma boundary can be estimated as  $1.5 \cdot 10^{-4}$  T [3].

In these tokamak discharges a dependence of the mode rotation on the mode amplitude is observed. The rotation takes place in the range of the mode amplitudes between the mode locking margins  $1.5 \cdot 10^{-4}$  T and  $11.5 \cdot 10^{-4}$  T. In other cases when the mode amplitude is lower than  $1.5 \cdot 10^{-4}$  T and higher than  $11.5 \cdot 10^{-4}$  T the mode rotation stops. This effect can be attributed to the mode locking by the permanent Error Field.

### Numerical Modelling

The TEAR code is based on the non-linear Rutherford model of the tearing mode in cylindrical approximation. The effect of the RMP of the same helicity as the tearing mode under consideration is taken into account.

The time evolution of the cosine and sine components of the helical magnetic flux perturbation  $\Psi = \Psi_C(r, t) \cos(m\theta - n\varphi) + \Psi_S(r, t) \sin(m\theta - n\varphi)$  at  $r = r_s$ , where  $q(r_s) = m/n$ , is described by the Rutherford equations:

$$\frac{d\Psi_C}{dt} = \pi a^2 \omega_R \frac{\Delta'_C(W)}{W} \Psi_C - \Omega_{rl} \Psi_S, \quad (1)$$

$$\frac{d\Psi_S}{dt} = \pi a^2 \omega_R \frac{\Delta'_S(W)}{W} \Psi_S + \Omega_{rl} \Psi_C. \quad (2)$$

In (1) and (2),  $\omega_R = 1/\tau_R$  is the inverse resistive time,  $\tau_R = \mu_0 a^2 / \eta$ . The stability parameters,  $\Delta'_C(W)$  and  $\Delta'_S(W)$ , for the cosine and sine components of the magnetic perturbation are obtained solving the equations (see [1 - 4]) for the helical magnetic flux,  $\Psi$ , radial distribution with account of the RMP. In (1) and (2),

$$\Omega_{rl} = mV_\theta / r_s - nV_\phi / R \quad (3)$$

is a parameter depending on the toroidal,  $V_\varphi$ , and poloidal,  $V_\theta$ , rotation velocities of the resonant plasma layer  $r_S - W/2 \leq r \leq r_S + W/2$ , where  $W$  is the width of the magnetic island. We use the equations of angular motion in the toroidal and poloidal directions to calculate the time variations of  $V_\varphi$  and  $V_\theta$ . We assume that the plasma inertial torque is balanced by the sum of the electromagnetic,  $M_{EM\varphi,\theta}$ , and viscous friction,  $M_{F\varphi,\theta}$ , torques:

$$\frac{I_\varphi}{R} \frac{dV_\varphi}{dt} = M_{EM\varphi} - M_{F\varphi}, \quad (4)$$

$$\frac{I_\theta}{r_S} \frac{dV_\theta}{dt} = M_{EM\theta} - M_{F\theta}. \quad (5)$$

In the equations (4) and (5),  $I_\varphi$  and  $I_\theta$  are the toroidal and poloidal moments of inertia of the resonant plasma layer.

The tearing mode rotation is described by equations (1) and (2). The mode rotation can be considered as the superposition of the resonant plasma layer rotation and the mode rotation with respect to this layer. According to the equations (4), (5), the RMP effect on the resonant plasma layer rotation increases with the growth of the mode amplitude because the electromagnetic torque is proportional to the mode amplitude. The high-amplitude mode locking conditions depend on the friction torques,  $M_{F\varphi,\theta}$ . The equations (1), (2) can be considered as the equations for an externally driven non-linear oscillator with the natural frequency  $\Omega_{rl}$ . The oscillator non-linearity is described by the dependences of  $\Delta'_{C,S}$  on the magnetic island width. The external driving force is expressed by the  $\Delta'_{C,S}$  dependences on the RMP. The  $\Delta'_{C,S}$  values depend on the RMP amplitude as well as on the shift between the mode angular position and the angular position of the RMP. The RMP effect on the mode rotation with respect to the resonant plasma layer should increase with a decrease of the mode amplitude because the strength of the  $\Delta'_{C,S}$  dependences on the RMP amplitude grows up with the decrease of the magnetic island width  $W$ . As the result, the equations (1), (2) describe the low-amplitude mode locking. The conditions of this locking depend on the value of the inverse resistive time,  $\omega_R$ .

The uncertainties of the used model relate to the calculation of the inverse resistive time and the friction torques. In our simulation of the tearing mode dynamics, the assumed values of  $\omega_R$  as well as the values of the toroidal and poloidal friction torques were scanned to find the required values by the comparison between the simulation results and the experimental data. The calculated dependences of the RMP value for the mode locking threshold on the assumed  $\omega_R$  and on the normalized friction forces are given with the red curves in Fig. 1 and Fig. 2. The calculations were made for the mode amplitudes equal to  $1.5 \cdot 10^{-4}$  T (Fig. 1) and  $11.5 \cdot 10^{-4}$  T (Fig. 2) that are equal to the experimental mode-locking margins of the mode amplitude.

In Fig. 1, one can see that the intersection between the RMP curve for the

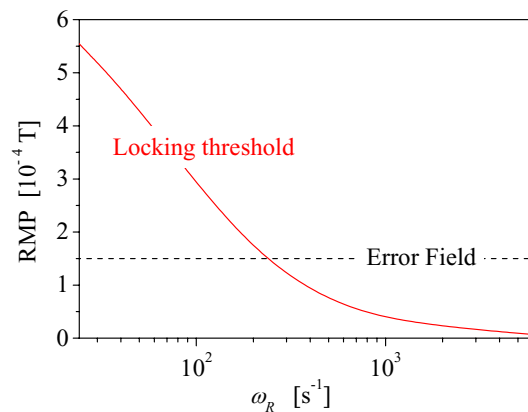


Fig. 1. The calculated dependence (red curve) of the threshold RMP value for the mode-locking on the assumed inverse resistive time  $\omega_R$ . The experimental Error Field value is shown with the black horizontal dashed line.

mode locking threshold and the experimental Error Field level takes place at  $\omega_R = 240 \text{ s}^{-1}$ . This  $\omega_R$  value corresponds to the assumption of the Spitzer plasma conductivity for the T-10 plasma periphery in the Ohmic regime with a strong MHD activity.

In Fig. 2, the black dashed curve specifies the combinations of the normalized toroidal and poloidal friction forces satisfying the condition of the mode locking threshold at the experimental Error Field level. The neoclassical values [10 - 12] of the toroidal and poloidal normalized friction forces for the T-10 conditions are shown with the black rectangle in Fig. 2. An overlapping of the rectangle and the black dashed curve means that the neoclassical viscosity can be considered as the physical mechanism that determines the required friction forces. In the following calculations we assume that the values of the normalized friction forces are  $2.7 \cdot 10^{-5} \text{ Nsm}^{-3}$  (toroidal) and  $1.6 \cdot 10^{-4} \text{ Nsm}^{-3}$  (poloidal).

According to the used model, the effect of the RMP on the mode rotation increases at sufficiently low and high mode amplitudes. It is illustrated by the result of the simulation given in Fig. 3. The dependence of the mode locking threshold value of the RMP on the mode amplitude is shown with the red curve in the top panel of Fig. 3. The threshold value decreases at sufficiently low and high mode amplitudes achieving the experimental Error Field level.

The calculations (see Fig. 3) were made for two cases of the assumed intrinsic rotation velocities of plasma outside the resonant layer in the toroidal,  $V_{0\phi}$ , and in the poloidal,  $V_{0\theta}$ , directions: the first case is a merely toroidal rotation, the second case is a merely poloidal rotation. It turned out that the RMP curves for the mode locking threshold coincide for these two cases. The locking of the low-amplitude mode is attributed to the  $\Delta'_{c,s}$  variations under influence of the RMP without significant changes of the resonant plasma layer rotation. The locking of the high-amplitude mode takes place because of appropriate changes in the resonant layer toroidal and poloidal rotation resulting in the reduction of the  $\Omega_{rl}$  absolute value. The dependences of the resonant layer toroidal and poloidal velocities on the mode amplitude are shown in the middle and bottom panels of Fig. 3 for the two cases of the plasma intrinsic rotation velocities.

### Summary

The TEAR code describes the experimentally observed locking of the tearing mode by a permanent Error Field in cases of low and high mode amplitudes. The used in the code resistive time corresponds to the plasma Spitzer conductivity. The friction forces affecting the rotation velocity of the resonant plasma layer relate to the plasma neoclassical viscosity. An exchange between the toroidal and poloidal momentums of the resonant layer takes place in the modelling due to the helicity of the mode and the RMP.

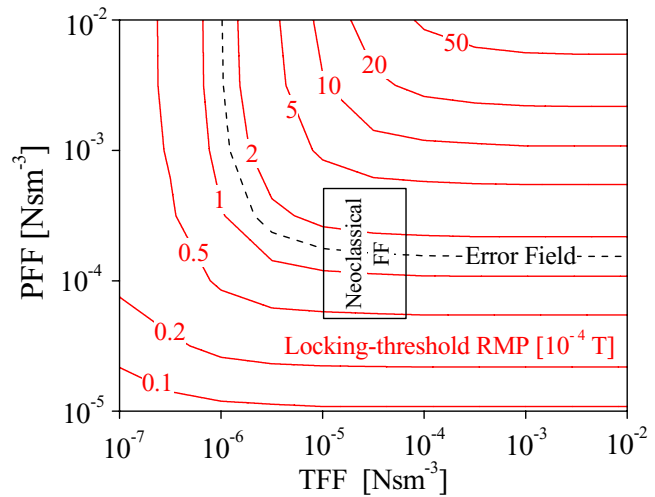


Fig. 2. The calculated dependence of the RMP value for the mode-locking threshold (red contour lines) on the toroidal (TFF) and poloidal (PFF) friction forces normalized to  $1 \text{ m}^2$  of resonant layer area and to  $1 \text{ m/s}$  difference between the velocities of the resonant layer and of the intrinsic rotation of the plasma outside the resonant layer. The locking threshold at the experimental Error Field value is shown with the black dashed line.

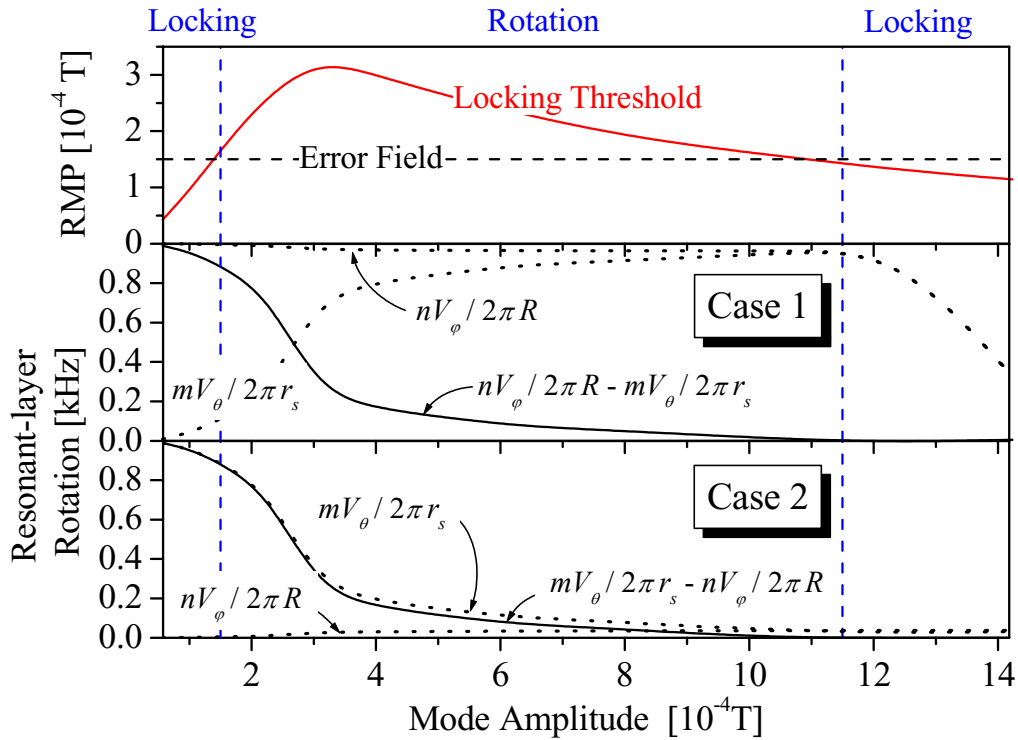


Fig. 3. The simulation results of the mode-locking conditions versus the mode amplitude: the calculated RMP value for the mode-locking threshold (red curve); resonant layer toroidal and poloidal velocities for two cases of intrinsic plasma rotation:

$$V_{0\phi}/2\pi R=1 \text{ kHz}, V_{0\theta}/2\pi r_s=0 \text{ (Case 1);}$$

$$V_{0\phi}/2\pi R=0, V_{0\theta}/2\pi r_s=0.5 \text{ kHz (Case 2).}$$

The experimental margins between the rotating-mode and the locked-mode amplitude values are shown with the blue vertical dashed lines. The experimental Error Field value is shown in the top panel with the black horizontal dashed line.

### Acknowledgments

We thank S.V.Konovalov, V.V.Piterskii and V.V.Poznyak for helpful discussions.

### References

1. A.N. Chudnovskiy, Yu.V. Gvozdkov, N.V. Ivanov et al. Nucl. Fusion, 43 (2003) 681.
2. A.N. Chudnovskiy, N.V. Ivanov, A.M. Kakurin et al. Nucl. Fusion, 44 (2004) 287.
3. N.V. Ivanov, A.M. Kakurin, I.I. Orlovskiy. 32<sup>nd</sup> EPS Conference on Plasma Physics, Tarragona, 27 June – 1 July 2005 ECA Vol.29C, P-5.068 (2005). <http://epsppd.epfl.ch/>
4. N.V. Ivanov, A.N. Chudnovskiy, A.M. Kakurin, I.I. Orlovskiy. 33<sup>rd</sup> EPS Conference on Plasma Physics, Rome, 19 – 23 June 2006 ECA Vol.301, P-1.176 (2006). <http://epsppd.epfl.ch/>
5. P.H. Rutherford. Phys. Fluids 16 (1973) 1903.
6. R.B. White, D.A. Monticello, M.N. Rosenbluth, et al. Phys.Fluids 20 (1977) 800.
7. M.F.F. Nave, J.A. Wesson. Nucl. Fusion, 30 (1990) 2575.
8. R. Fitzpatrick. Nucl. Fusion, 33 (1993) 1049.
9. R. Fitzpatrick. Phys. Plasmas, 5 (1998) 3325.
10. T.H.Stix. Phys. Fluids 16 (1973) 1260.
11. A.B.Hassam, R.M.Kulsrud. Phys. Fluids 21 (1978) 2271.
12. T.H.Jensen, A.W.Leonard, A.W.Hyatt. Phys. Fluids B 5 (1993) 1239.